

Pibo Ma,
Gaoming Jiang,
*Fa Zhang,
Qing Chen,
Xuhong Miao,
Honglian Cong

College of Textile and Clothing,
Jiangnan University,
Wuxi 214122, China

*College of Textiles,
Donghua University,
Shanghai 201620, China

Corresponding author
Ma P. E-mail: mapibo@jiangnan.edu.cn
Jiang G. E-mail: Jiang@526.cn

Experimental Investigation on the Compression Behaviours of 3D Angle-interlock Woven Composites with Carbons Nanotube under High Strain Rates

Abstract

The compressive properties of 3D angle-interlock woven/epoxy resin composites with various carbon nanotube (CNTs) contents were investigated under quasi-static and high strain rate loading to evaluate the compressive failure modes, which were influenced by various CNT contents and different strain rates. The results indicated that the stress strain curves were strain rate sensitive, and the compressive failure stress of composites with various CNT contents were increased with a change the strain rates and CNT contents. The compressive failure modes of 3D angle-interlock woven composites without CNT tended to be in shear deformation, delamination fibre breakage and matrix crack together, and the failure modes of 3D angle-interlock woven composites with high CNT contents presented delamination and shear deformation.

Key words: 3D angle-interlock woven composites, carbon nanotubes (CNTs), impact compression behaviours, high strain rates,

Introduction

Textile structural composites have become more popular nowadays because of their lower cost and excellent structures. They have high stiffness and high resistance to corrosion and abrasion [1]. However, the strain rate is a sensitive element that influences the dynamic strength, such as the compression, tension and failure strain of textile structural composites. Many researchers have investigated the dynamic strength of these composites within the strain rate range they needed.

Carbon nanotubes (CNTs) offer a new opportunity to enhance the mechanical properties of fibre reinforced composites simply due to their excellent Young's modulus and strength, high aspect ratio, large surface areas and excellent thermal properties. Thakre et al. [2] prepared epoxy/single walled carbon nanotubes/carbon woven composites and tested their mechanical properties. The results indicated that the interlaminar shear strength was improved by employing functionalised nanotubes. Grimmer and Dharan [3] researched the fatigue properties of carbon nanotube reinforced glass fibre/polymer composites. They found that the fatigue properties of the carbon nanotube reinforced composite was improved compared with conventional matrix composites. Tsantzalís et al. [4] mixed carbon nanofibres (CNF) into epoxy resin and studied the mechanical quasi-static properties influenced by the ingredient added. Besides this the reinforcement of the mechanical properties were observed after the addition of the CNF. Wichmann et al. [5] studied the mechanical properties of

glass fibre reinforced composites with a nanotube modified matrix. They found that the interlaminar shear strengths of the nanotubemodified composites were significantly improved (16%) by adding only 0.3 wt% of carbon nanotubes. Romhany and Szebenyi [6] filled epoxy resin with multiwalled carbon nanotubes (MWCNTs) and prepared MWCNT/carbon fibre/epoxy composites. The interlaminar fracture toughness values were observed to obviously increase in their study. Yokozeki et al. [7] analysed the mechanical behaviours of CFRP laminates manufactured from unidirectional prepreps with cup-stacked carbon nanotube (CSCNT)-dispersed epoxy, and noted that the improvement in stiffness and strength and no adverse influences on mechanical properties were experimentally verified due to the dispersion of CSCNT. Siddiqui et al. [8] observed the tensile strength of glass fibres with carbon nanotube-epoxy nanocomposite coating. The results showed that the tensile strength of single fibres obviously increased with increasing carbon nanotube content up to a certain level. Solima et al. [9] studied the low-velocity impact of thin woven carbon fabric composites incorporating multi-walled carbon nanotubes (MWCNTs), and observed that the functionalised MWCNTs enhanced the impact response and limited the damage size in the woven carbon fibre composites. Meanwhile the addition of 1.5% MWCNTs resulted in a 50% increase in energy absorption. Kim et al. [10] studied the mechanical properties of multiwalled carbon nanotube (MWCNTs)-loaded plain-weave glass/epoxy composites, and found that the plain-weave com-

posites containing MWCNTs presented improved matrix-dominant and interlaminar fracture-related properties. Fan et al. [11] investigated the interlaminar shear strength of glass fibre reinforced epoxy composites enhanced with multi-walled carbon nanotubes (MWCNTs), and found that there was an increase in the interlaminar shear strength of up to 33% with adding the MWCNTs into the composite. As well as the preferential orientation of the MWCNTs, the thickness direction was found to contribute to the increase in the interlaminar shear properties. Qiu et al. [12] employed carbon nanotube integrated multifunctional multiscale composites. They found that the mechanical properties of the multiscale composites were remarkably enhanced. Davis and Whelan [13] researched the interlaminar shear fracture toughness of a nanotube reinforced composite. The results presented that the interlaminar shear toughness was obviously improved by the carbon nanotubes. Jindal et al. [14] discussed the high strain rate of MWCNT/polycarbonate composites. The research results revealed that the mechanical properties and energy absorption increased rapidly compared with the data of pure polycarbonate. Bhardwaj et al. [15] investigated the flexural and dynamic response of CNTs reinforced laminated composite plates. They found that the CNT contents and their aspect ratio had an obvious influence on the non-linear flexural and dynamic response of the laminated composite. Borbon et al. [16] observed the dynamic behaviours of composite sandwich plates with carbon nanotubes subjected to blast loading. The results indicated that the permanent displacement

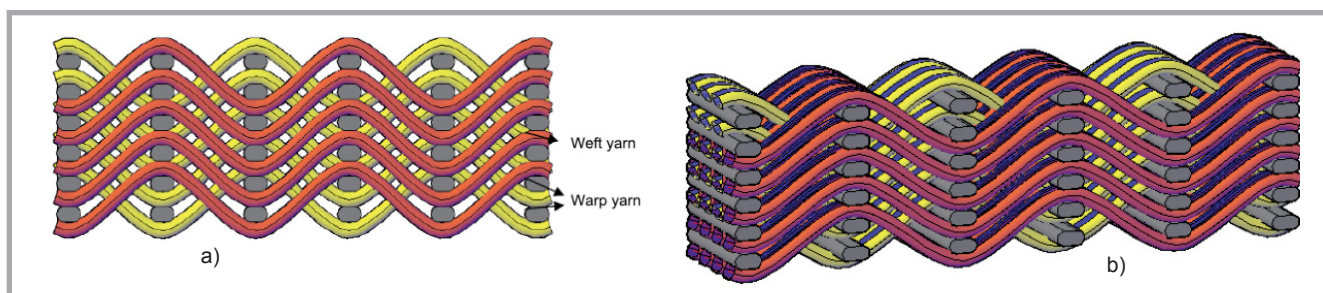


Figure 1. Weave structure of 3D angle-interlock woven fabric [19]; a) two-dimensional view, b) three-dimensional view.

was larger for the plates with CNTs; the inherent brittleness of epoxy resins was overcome by adding CNTs, and the failure load was larger for the specimens with CNTs. Fernandez et al. [17] investigated the influence of multiwall carbon nanotubes on the in-plane shear behaviour of epoxy glass fibre reinforced composites. The research evaluated the initial shear modulus and deterioration of the shear modulus during plastic, deformation and material hardening, but incorporating MWCNT into the resins did not affect the parameters investigated under the conditions imposed. Ma et al. [18] studied the transverse impact behaviours of glass warp-knitted fabric/foam sandwich composites through carbon nanotube incorporation and found that there was an increase in the impact velocity with an increase in the carbon nanotube content.

The compression behaviours of fibre reinforced composites at high strain rates are identified as impact compression. The impact compression behaviours change with a variation in the strain rates, which are also called the high strain rate effects of the composites. Textile structural composites are often employed in impulsive loadings, and the compression behaviour is a basic parameter for the design of composites. Moreover the impact compression behaviours of many types of composites show the strain rate effect. The strain rate effects of fibres and the polymer matrix are significant elements for the fibre reinforced composite design. Many researchers have discussed the impact behaviours of fibre reinforced composites with various CNT contents. Kostopoulos et al. [19] found about 0.5 wt% of MWCNTs can dispersed in the epoxy matrix of CFRP quasi-isotropic laminates subjected to a low velocity impact, and high CNT contents were beneficial for the impact damage and residual properties of the composites. Their impact often represents a low-velocity impact via a drop-weight; this kind of impact indicates low strain rates.

Fibre reinforced composites with CNTs are often employed with impulsive and impact loading, which means high strain rate loading. The dynamic behaviours and failure modes of fibre reinforced composites with CNTs are much different between lower and higher strain rate loading. It is necessary to analyse the mechanical behaviours and failure modes of carbon-nanotube fibre reinforced composites under higher strain rates of loading. However, the impact properties of fibre reinforced composites with CNTs under high strain rates are still beyond our scope. In the present study, a composite with CNTs added to resin was prepared. The strain rate effect of 3D angle-interlock woven composites with various CNT contents under impact compression was analysed.

Experimental methods

Materials

3D angle-interlock woven fabrics were prepared at the College of Textile and Clothing of Jiangnan University. The glass yarns were supplied by Taishan Glass Fibre Co. Ltd, whose glass yarn diameter was 168 tex in the warp direction and 254 tex in the weft direction, and each yarn contained 90 and 128 fibres, respectively. **Figure 1** shows a sample and structure of the 3D angle-interlock woven fabric [20, 21]. Glass filament tows without twists were used to weave the 3D angle-interlock fabric. Two adjacent layers of weft yarns were joined together by weaving the warp yarns. **Table 1** shows specifications of the fabric. The structural feature imparted both higher stiffness and strength to the thickness and in-plane directions.

Table 1. Specifications of the 3D angle-interlock woven fabric.

Yarns	Weaving density, ends/cm	Linear density, tex	Layers
Warp	8	168	6
Weft	4	254	5

The epoxy resin was Type 618, obtained from the Shanghai Resin Factory of China, with a tensile modulus of 1.97 GPa and tensile strength of 68.10 MPa. The type of MWCNTs was MFG 110413, supplied by Chengdu Organic Chemicals Co.Ltd., Chinese Academy of Sciences. The outer diameter (OD) of the MWCNTs was 10 - 20 nm, the length 10 - 30 μm and the purity was greater than 95 wt%.

Preparation of MWCNT-filled epoxy resin

The MWCNTs were dispersed in acetone solution. The concentration of the MWCNTs was 1 wt%. To get a homogenous solution, the mixture was ultra sonicated by an ultrasonic cell disruptor for about 6 hours at a supersonic frequency of 80 kHz. Then epoxy resin part A was added to the solution and stirred at 40 $^{\circ}\text{C}$ for 12 hours (The acetone was volatilized completely), while epoxy part B was added to the solution before fabricating the composites.

Composite fabrication

Composites were fabricated with MWCNT-filled epoxy resin by employing vacuum-aided resin transfer molding (VARTM) technology. The void content of the composites was less than 1% and the fibre volume fraction was approximately 40%. The fibre volume fraction was approximately 40% and the void content less than 1%. The void content was measured by the following equation:

$$V_v = [1 - \rho_s(w_f/\rho_f + w_r/\rho_r)] \times 100\% \quad (1)$$

where, V_v is the void content, ρ_s the density of the composite in kg/m^3 , w_f and w_r the mass fraction of carbon fabrics and

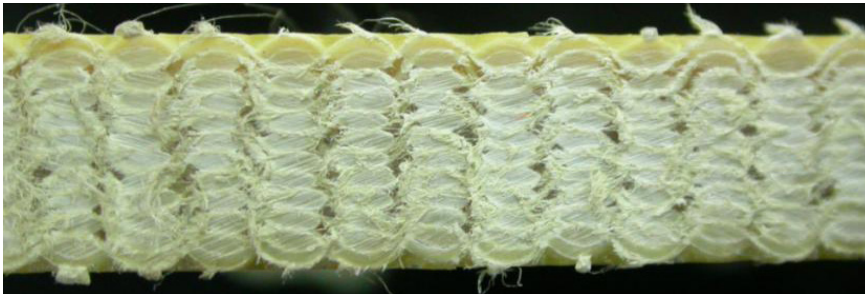


Figure 2. Cross-section of 3D angle-interlock woven composites [20].

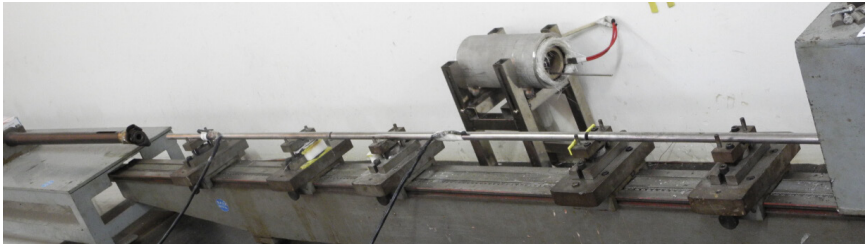


Figure 3. Set up of split Hopkinson pressure bar.

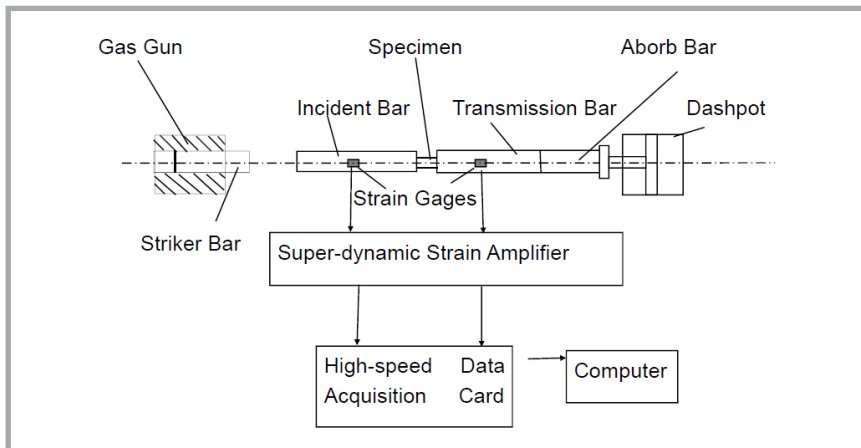


Figure 4. Schematic of split Hopkinson pressure bar.

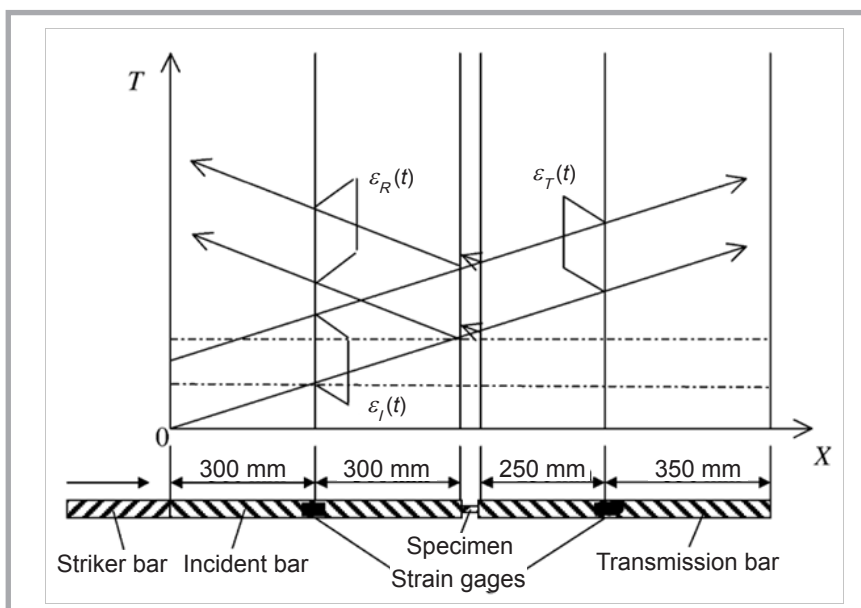


Figure 5. Principle of split Hopkinson pressure bar [22].

resin, respectively, and ρ_f and ρ_r are the density of carbon fabrics and resin, respectively in kg/m^3 .

The size of the composites is dependent on the mould, being about 200×200 mm (length \times width). Figure 2 is the cross-section of 3D angle-interlock woven composites [20].

Compression tests under various strain rates

Compression tests were conducted under both quasi-static and high strain rates. A compression test under the quasi-static condition was performed on an MTS810.23 system at a speed of 1 mm/min. The size of specimen was 9×9 mm (length \times width), which is dependent on the characteristics of the split Hopkinson pressure bar (SHPB) apparatus.

The high strain rates compression tests were carried out on SHPB apparatus. A schematic illustration and principle of the SHPB are shown in Figure 3. A specimen is placed between two elastic bars of the same cross sectional area and modulus, which are separately identified as the incident bar and transmission bar. The material of the striker and pressure bars made of steel are subjected to maraging at extremely high yield strength in order to withstand a very high impact velocity. An elastic stress pulse is imparted to the incident bar by impacting it with a striker bar of the same cross sectional area and modulus. The impact of the striker bar generates an elastic stress wave equal to twice the length of the striker bar, which then propagates through the incident bar at the speed of sound in the bar media and passes through the specimen while deforming it. The particle velocity imparted to the incident bar is half the impact velocity of the striker bar. The stress in the bar is given by

$$v = \rho C_0 v_p \quad (2)$$

where, ρ is the density of the bar material, C_0 the bar velocity and v_p is the particle velocity.

When the elastic wave reaches the specimen-incident bar interface, part of it will be reflected back, and part will be transmitted through the specimen and pass through the transmission bar. To obtain the direct incident pulse, reflected pulse and transmitted pulse, strain gauges are mounted on both the incident and trans-

mitter bars. One-dimensional wave propagation is assumed to analyse the strain signals from the strain gauges, where E_b , A_b and ρ_b represent the modulus, cross section area and density of the bar and E_s , A_s and ρ_s mean those of the specimen. The equations for the strain rates ($\dot{\varepsilon}$), strain (ε) and stress (σ) of the specimen are as follows:

$$\dot{\varepsilon}(t) = -\frac{2C_0}{L_s} \varepsilon_R(t) \quad (3)$$

$$\varepsilon(t) = -\frac{2C_0}{L_s} \int_0^t \varepsilon_R(t) dt \quad (4)$$

$$\sigma(t) = \frac{E_b A_b}{A_s} \varepsilon_T(t) \quad (5)$$

where, t is the time, $C_0 = \sqrt{E_b/\rho_b}$ the longitudinal wave velocity in the bar and L_s refers to the specimen length $\varepsilon_R(t)$ and $\varepsilon_T(t)$ are the strain gauge signals of the reflected and transmitted pulses, respectively.

The function of time and average stress and strain in the specimen can be calculated and the mechanical properties of the composite, such as strain rates and stress-strain behaviour, along loading direction can be deduced from *Equations 3 - 5*.

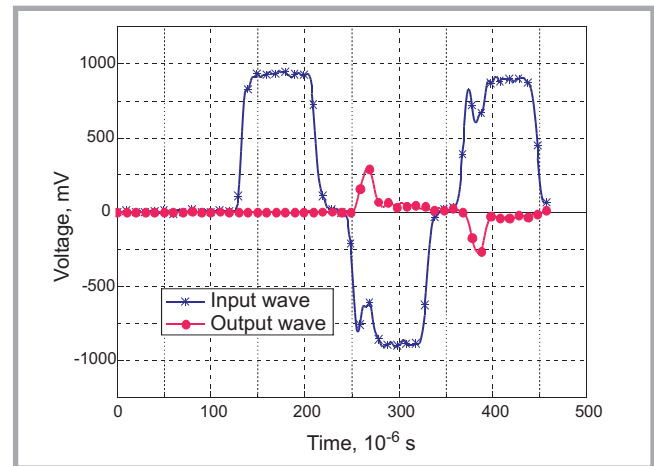
A gas gun of 14.5 mm inner diameter was employed in this study as a momentum trapping device equipped onto the SHPB, with the incident and transmission bars having the same diameter (diameter 14.5 mm and length 600 mm). Compressed nitrogen gas was employed to operate the gas gun and propel the strike bar to move a distance of 200 mm. The impact velocity of the gas gun (strike bar) could be altered by changing the gas pressure to get the strain rates required. *Figures 3 and 4* display the schematic and principle of splitting the Hopkinson pressure bar, respectively, and *Figure 5* is the principle of split Hopkinson pressure bar [22].

Results and discussion

Stress-strain relations

Compression tests of composites with various CNT contents were implemented at different strain rates, and at least five samples were tested at each strain rate (including the quasi-static state). Several typical signals obtained from the input and output bars under various CNT content conditions are shown in *Figure 6*. According to the one dimensional stress wave propagation theory of SHPB apparatus, the stress strain curves at high

Figure 6. Typical signals in input and output bar with 1.5 wt% CNTs at a strain rate of 1600/s.



strain rates can be calculated, the results of which are displayed in *Figure 7 - 10*. It is obvious that the strain rate with different CNT contents influences the stress-strain curves a lot, which appears at each of the strain rates, including quasi-static and high strain rate loading. The compressive failure stress rises with an increase in the strain rate and CNT content, meanwhile, the compressive failure strain decreases with an increase in the strain rate and CNT content.

The stress-strain curves of 3D angle-interlock woven fabric composites without CNTs at various strain rates are shown in *Figure 7*, indicating an obvious increase in the compressive failure stress, and the failure strain decreases with an increase in the strain rate. The compression properties of the 3D angle-interlock woven composite is determined by the mechanical behaviours of glass fibres in the woven structure and by the resin. As the glass fibre and resin are both strain rate sensitive, the stress-strain curves of the 3D angle-interlock composite are also such. The stress-strain curve during quasi static compression shows lower compressive stiffness, which increases when the strain rate rises.

The stress-strain curves of woven fabric composites with 0.5wt% CNTs at various strain rates are displayed in *Figure 8*. For the composites without CNTs, *Figure 7* is similar in that the compressive failure stress increases with an increase in the strain rate, while the compressive failure strain decreases with an increase in the strain rate, indicating that the composite with CNTs is also strain rate sensitive. Comparing the composites without CNTs, their failure stress with CNTs is much larger than that of composites without CNTs, which is because CNTs can

improve the interface strength between the fibres and resin. However, what is peculiar is that the compressive stiffness of composites with 0.5 wt% CNTs under various strain rates is much lower than that of composites without CNTs, the reason for which is that CNTs increase the plasticity property of the resin, indicating that the composites with CNTs can absorb more energy under impact compression loading.

The stress-strain curves of 3D angle-interlock woven fabric composites with 1.0 wt% CNTs and 1.5wt% CNTs at various strain rates are shown in *Figure 9 - 10* respectively. Similar to *Figure 8*, the compressive failure stress grows with an increase in both the strain rate and CNT contents, while the compressive failure strain declines when the strain rate increases. At the same time the compressive stiffness of composites with CNTs is lower than for composites with a lower CNT content.

It can be seen from *Figure 7 - 10* that the failure stress, strain and stiffness of 3D angle-interlock woven composites is significantly influenced by the CNT content.

Mechanical properties

The compressive failure stress and failure strain of 3D angle-interlock woven composites with various CNTs under different strain rates are shown in *Figures 11 - 12*. It can be noticed that the compressive failure stress shows a linear increase with the strain rate and CNT contents, and the compressive failure strain decreases linearly with the strain rate and CNT contents. The failure strains at higher strain rates and at higher CNT contents are obviously decreased compared with those in quasi-static compression and those of composites without CNTs. Firstly it can

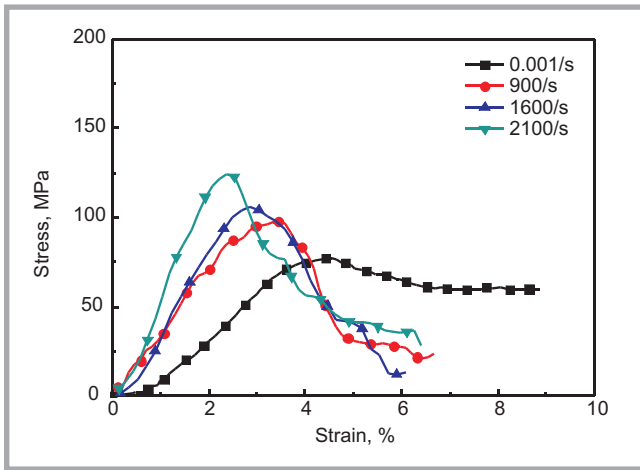


Figure 7. Stress-strain curves of 3D angle-interlock woven fabric composites with CNTs (0 wt%) at various strain rates.

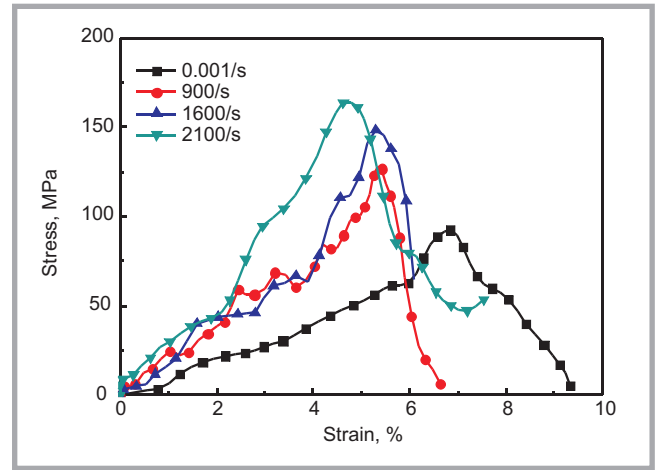


Figure 8. Stress-strain curves of 3D angle-interlock woven fabric composites with CNTs (0.5 wt%) at various strain rates.

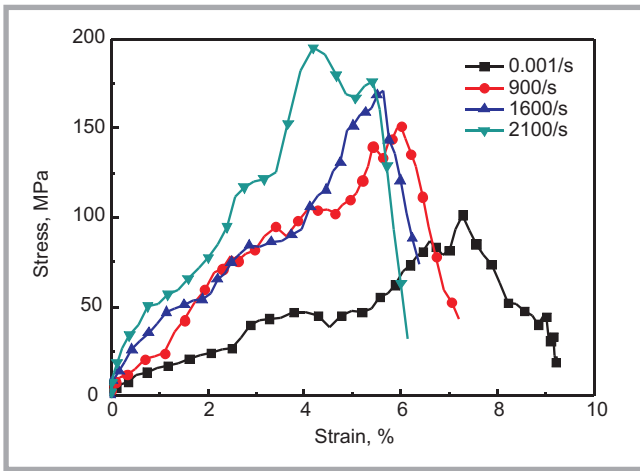


Figure 9. Stress-strain curves of 3D angle-interlock woven fabric composites with CNTs (1.0 wt%) at various strain rates.

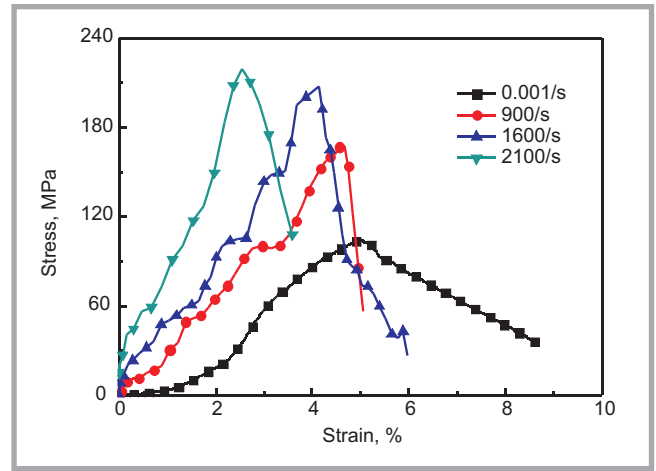


Figure 10. Stress-strain curves of 3D angle-interlock woven fabric composites with CNTs (1.5 wt%) at various strain rates.

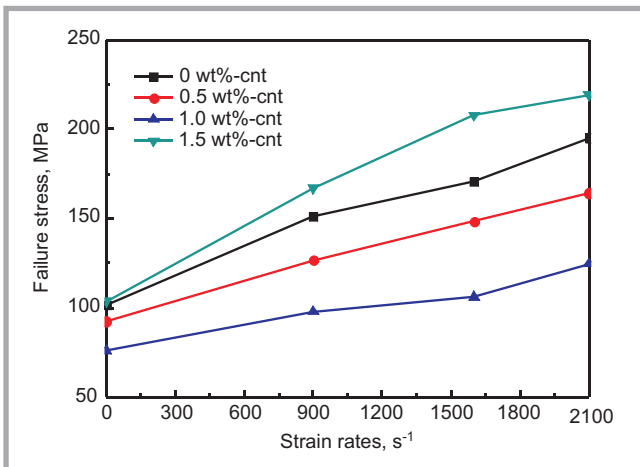


Figure 11. Failure stress of 3D angle-interlock woven fabric composites with different contents of CNTs at various strain rates.

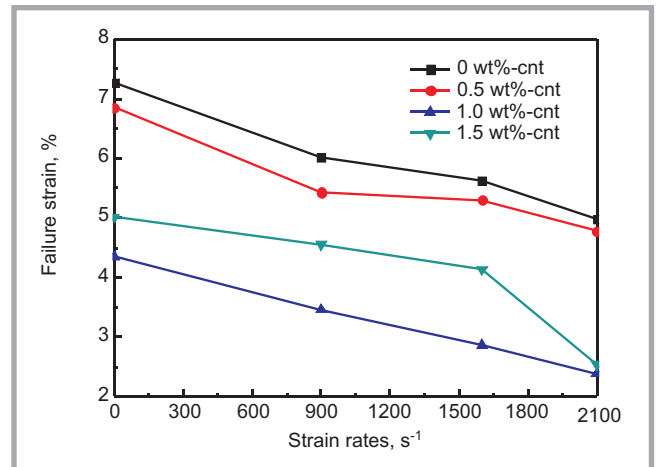


Figure 12. Failure strain of 3D angle-interlock woven fabric composites with different contents of CNTs at various strain rates.

be attributed to compression damage occurring during quasi static compression, propagating more slowly than that under high strain loading. This induces the failure of the reinforcement phase

(3D angle-interlock woven fabric) in the through thickness direction, which includes deformation. Under higher strain rate compression, the impulsive loadings induce matrix cracking and breaking of

the interlaminar yarns. Secondly the CNTs can increase the plasticity property of resin, and the deformation property of resin/CNTs can be obviously improved with a higher CNT content. The failure

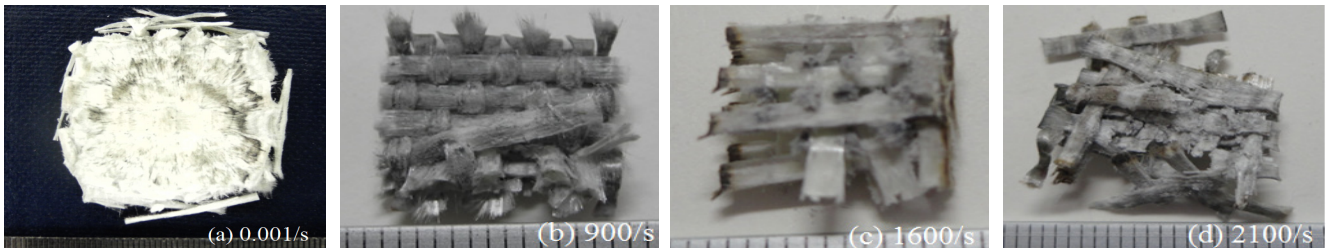


Figure 13. Compression fractures of 3D angle-interlock woven fabric composites with CNTs (0 wt%) at various strain rates.

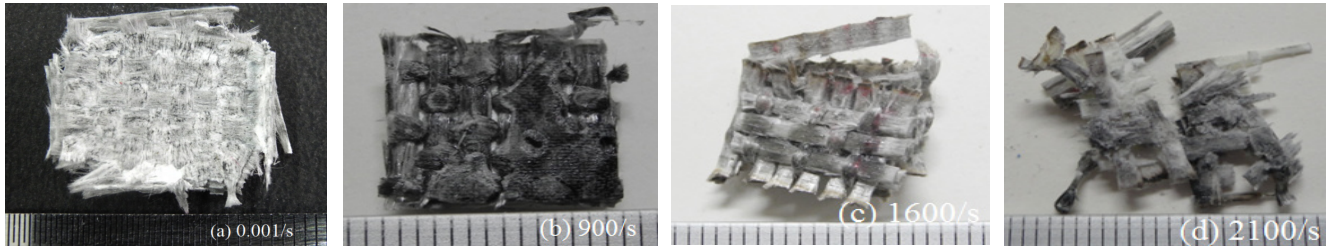


Figure 14. Compression fractures of 3D angle-interlock woven fabric composites with CNTs (0.5 wt%) at various strain rates.

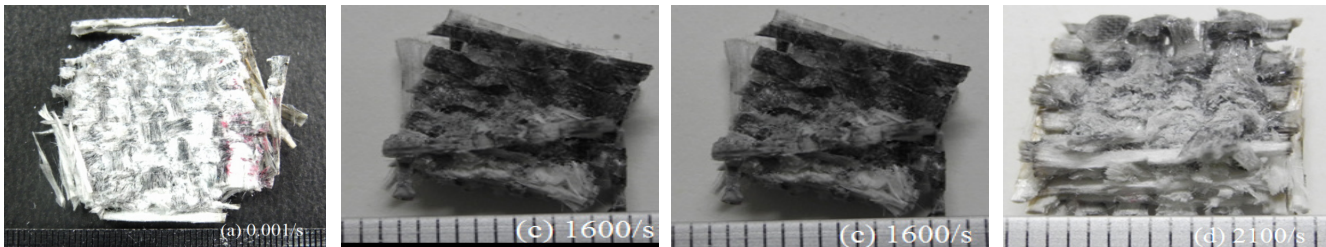


Figure 15. Compression fractures of 3D angle-interlock woven fabric composites with CNTs (1.0 wt%) at various strain rates.

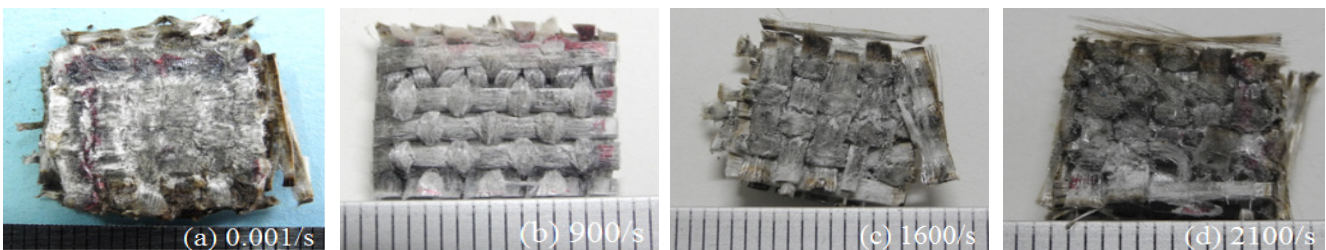


Figure 16. Compression fractures of 3D angle-interlock woven fabric composites with CNTs (1.5 wt%) at various strain rates.

strain can be larger when the composites have a higher CNT content under impact compression loading.

Compression fracture features

The fracture characteristics of 3D angle-interlock woven composites without CNTs at various strain rates are illustrated in the photographs of **Figure 13**. It can be observed that both fibre breakage and shear deformation occur at different strain rates and the main damage mode is shear failure. **Figure 13** shows that when the strain rate increases, the composites are compressed almost into debris. During quasi static compression, this manifests shear failure among the angle-interlock woven under a higher stress than the matrix strength. As the strain increases,

angle-interlock woven breakage accompanied with the shear occurs. With a growth in the strain rate, the whole composite sample turns into debris because of the difference in stress wave velocity between the reinforcement and matrix, which is also due to the higher energy rate applied to the composite sample.

Figure 14 displays the damage modes of 3D angle-interlock woven composites with 0.5 wt% CNTs at various strain rates under compression loading. Similar the failure states of composites without CNTs, the fibre breakage, delamination and shear deformation occur jointly under various strain rates. And the delamination under high strain rates, such as

2100/s, is the main failure mode of composites.

Figure 15 illustrates the failure modes of woven composites with 1.0 wt% CNTs at various strain rates under compression loading. It is distinct that the failure modes in both a quasi-static state and at high strain rates are quite different. Both matrix cracking and fibre breakage under quasi-static compression are the main failure modes. However, a matrix crack only occurs under high strain rates.

Figure 16 shows the failure modes of woven composites with 1.5 wt% CNTs at various strain rates under compression loading. It can be observed that matrix cracking is still the main failure mode.

The damage of composites with high CNT contents is distinct for composites with low CNT contents and without CNTs, the reason for which is the high content of CNTs, leading to an increase in roughness of the composites, and consequently they absorb more energy with smaller deformation.

Conclusions

The impact compression, including quasi-static and high strain rate compression, properties of 3D angle-interlock woven/epoxy resin composites with various CNT contents (0, 0.5, 1.0 and 1.5 wt %) were investigated using an MTS mechanical tester and split Hopkinson pressure bar (SHPB) respectively. Compression stress vs. strain curves of the 3D angle-interlock woven composites with various CNT contents were obtained and a comparative analysis carried out. The stress strain curves are strain rate sensitive. The failure stress increases with a rise in strain rates and CNT contents, while the failure strain decreases with rise in the strain rates and CNT contents. The compressive failure stress is increased with a rise in strain rates. Fracture images of the damage of composites with different CNT contents at various strain rates indicate the existence of fibre breakage, matrix cracking, delamination and shear deformation modes during the test of the composites without CNTs under various strain rates, whereas there are only matrix cracking and delamination failure modes for composites with high CNT contents. The CNTs do increase the energy absorption of the composites because they can enhance their roughness efficiently. The mechanical parameters of composites with CNT contents at high strain rates obtained can benefit the design of the composite's structures.

References

- Ma P, Gao Z. A review on the impact tension behaviours of textile structural composites. *Journal of Industrial Textiles*. 2013; 1528083713503001.
- Thakre PR, Lagoudas DC, Riddick JC, Gates TS, Frankland S-JV, Ratcliffe JG, et al. Investigation of the effect of single wall carbon nanotubes on interlaminar fracture toughness of woven carbon fibre-epoxy composites. *Journal of Composite Materials*. 2011; 45(10): 1091-107.
- Grimmer CS, Dharan C. Enhancement of delamination fatigue resistance in carbon nanotube reinforced glass fibre/polymer composites. *Composites Science and Technology*. 2010; 70(6): 901-8.
- Tsantzalis S, Karapappas P, Vavouliotis A, Tsoira P, Paipetis A, Kostopoulos V, et al. Enhancement of the mechanical performance of an epoxy resin and fibre reinforced epoxy resin composites by the introduction of CNF and PZT particles at the microscale. *Composites Part A: Applied Science and Manufacturing*. 2007; 38(4):1076-81.
- Wichmann MHG, Sumfleth J, Gojny FH, Quaresimin M, Fiedler B, Schulte K. Glass-fibre-reinforced composites with enhanced mechanical and electrical properties-Benefits and limitations of a nanoparticle modified matrix. *Engineering Fracture Mechanics*. 2006; 73(16): 2346-59.
- Romhány G, Szebenyi G. Interlaminar crack propagation in MWCNT/fibre reinforced hybrid composites. *Express Polym Lett*. 2009; 3(3): 145-51.
- Yokozeki T, Iwahori Y, Ishiwata S, Enomoto K. Mechanical properties of CFRP laminates manufactured from unidirectional prepregs using CSCNT-dispersed epoxy. *Composites Part A: Applied Science and Manufacturing*. 2007; 38(10): 2121-30.
- Siddiqui NA, Sham ML, Tang BZ, Munir A, Kim JK. Tensile strength of glass fibres with carbon nanotube-epoxy nanocomposite coating. *Composites Part A: Applied Science and Manufacturing*. 2009; 40(10): 1606-14.
- Soliman E, Shyka M, Taha MR. Low-velocity impact of thin woven carbon fabric composites incorporating multi-walled carbon nanotubes. *International Journal of Impact Engineering*. 2012; 47: 39-47.
- Kim MS, Lee SE, Lee WJ, Kim CG. Mechanical Properties of MWNT-Loaded Plain-Weave Glass/Epoxy Composites. *Advanced Composite Materials*. 2009; 18(3): 209-19.
- Fan Z, Santare MH, Advani SG. Interlaminar shear strength of glass fibre reinforced epoxy composites enhanced with multi-walled carbon nanotubes. *Composites Part A: Applied Science and Manufacturing*. 2008; 39(3): 540-54.
- Qiu J, Zhang C, Wang B, Liang R. Carbon nanotube integrated multifunctional multiscale composites. *Nanotechnology*. 2007; 18: 275708.
- Davis DC, Whelan BD. An experimental study of interlaminar shear fracture toughness of a nanotube reinforced composite. *Composites Part B: Engineering*. 2011; 42(1): 105-16.
- Jindal P, Pande S, Sharma P, Mangla V, Chaudhury A, Patel D, et al. High Strain Rate Behaviour of Multi-Walled Carbon Nanotubes-Polycarbonate Composites. *Composites Part B: Engineering*. 2013; 45(1): 417-422.
- Bhardwaj G, Upadhyay A, Pandey R, Shukla K. Non-linear flexural and dynamic response of CNT reinforced laminated composite plates. *Composites Part B: Engineering*. 2013; 45(1): 89-100.
- Borbón F, Ambrosini D. Dynamic response of composites sandwich plates with carbon nanotubes subjected to blast loading. *Composites Part B: Engineering*. 2013; 45(1): 466-473.
- Fernández C, Medina C, Pincheira G, Canales C, Flores P. The effect of multiwall carbon nanotubes on the in-plane shear behaviour of epoxy glass fibre reinforced composites. *Composites Part B: Engineering*. 2013; 55: 421-425.
- Ma P, Zhang F, Jiang G, Zhu Y. Transverse impact behaviours of glass warp-knitted fabric/foam sandwich composites through carbon nanotubes incorporation. *Composites Part B*. 2014; 56(1): 847-856.
- Kostopoulos V, Baltopoulos A, Karapappas P, Vavouliotis A, Paipetis A. Impact and after-impact properties of carbon fibre reinforced composites enhanced with multi-wall carbon nanotubes. *Composites Science and Technology*. 2010; 70(4): 553-63.
- Jin L, Sun B, Gu B. Finite element simulation of three-dimensional angle-interlock woven fabric undergoing ballistic impact. *Journal of The Textile Institute*. 2012; 102(11): 982-993.
- Jin L, Hu H, Sun B, Gu B. Three-point bending fatigue behaviour of 3D angle-interlock woven composite. *Journal of Composite Materials*. 2011; 46(8): 883-894.
- Ma P, Jiang G, Chen Q, Miao X, Zhao S. Compression behaviours of carbon nanotube-filled epoxy resin under high strain rates. *Textile Research Journal*. 2014; 10.1177/0040517514540768

Acknowledgment

The authors acknowledge the financial support of the National Science Foundation of China (No. 11302085), the National Science and Technology Support Program of China (No. 2012BAF13B03) and the Fundamental Research Funds for the Central Universities (No. JUSRP51404A and No. JUSRP1043).

Received 24.04.2014 Reviewed 03.07.2014